

Observation of the cluster spin-glass phase in $\text{La}_{2-x}\text{Sr}_x\text{CuO}_4$ by anelastic spectroscopy

F. Cordero

*CNR, Area di Ricerca di Tor Vergata, Istituto di Acustica "O.M. Corbino",
Via del Fosso del Cavaliere 100, I-00133 Roma, and INFM, Italy*

R. Cantelli, A. Paolone

*Università di Roma "La Sapienza", Dipartimento di Fisica, P.le A.
Moro 2, I-00185 Roma, and INFM, Italy*

M. Ferretti

*Università di Genova, Dipartimento di Chimica e Chimica Fisica,
Via Dodecanneso 31, I-16146 Genova, and INFM, Italy*

An increase of the acoustic absorption is found in $\text{La}_{2-x}\text{Sr}_x\text{CuO}_4$ ($x = 0.019, 0.03$ and 0.06) close to the temperatures at which freezing of the spin fluctuations in antiferromagnetic-correlated clusters is expected to occur. The acoustic absorption is attributed to changes of the sizes of the quasi-frozen clusters induced by the vibration stress through magnetoelastic coupling.

I. INTRODUCTION

The low doping region of the phase diagram of $\text{La}_{2-x}\text{Sr}_x\text{CuO}_4$ is attracting considerable interest, due to the appearance of unconventional correlated spin dynamics and ordering processes (for a review see Ref. 1). In undoped La_2CuO_4 the Cu^{2+} spins order into a 3D antiferromagnetic (AF) state with the staggered magnetization in the ab plane.² Doping by Sr rapidly destroys the long range AF order, with T_N passing from 315 K to practically 0 K around $x_c \simeq 0.02$. Above this critical value of the Sr content no long range AF order is expected at finite temperature. There are also indications that the holes are segregated into domain walls, sometimes identified as charge stripes, which separate hole-poor regions where the AF correlations build up.^{3,4} The holes should be mobile along these "charge rivers", but at low x they localize near the Sr atoms below ~ 30 K, causing a distortion of the spin texture of the surrounding Cu^{2+} atoms.⁴ For $x < x_c$ the spin distortions around the localized holes are decoupled from the AF background, and freeze into a spin-glass (SG) state below $T_f(x) \simeq (815 \text{ K})x$. For $x > x_c$ a cluster spin-glass (CSG) state is argued to freeze below $T_g(x) \propto 1/x$ and AF correlations develop within the domains defined by the charge walls, with the easy axes of the staggered magnetization uncorrelated between different clusters. The formation of the SG and CSG states are inferred from sharp maxima in the ^{139}La NQR^{3,1,5} and μSR ⁶ relaxation rates, which indicate the slowing of the AF fluctuations below the measuring frequency ($\sim 10^7 - 10^8$ Hz in those experiments) on cooling, and from the observation of irreversibility, remnant magnetization, and scaling behavior in magnetic susceptibility experiments.^{7,8}

Here we report the observation of a step-like increase of the low-frequency acoustic absorption close to the temperature at which the spin freezing process is detected in the NQR measurements. The absorption is ascribed to changes of the sizes of the frozen clusters induced by the vibration stress through magnetoelastic coupling,⁹ or equivalently to the motion of the walls between them.

II. EXPERIMENTAL AND RESULTS

The samples were prepared by standard solid state reaction as described in Ref. 10 and cut in bars approximately $40 \times 4 \times 0.6 \text{ mm}^3$. The final Sr contents and homogeneities were checked from the temperature position and sharpness of the steps in the Young's modulus and acoustic absorption due to the tetragonal (HTT) / orthorhombic (LTO) transition, which occurs at a temperature T_t linearly decreasing with doping.¹¹ The transitions appear narrower in temperature than the one of a Sr-free sample, indicating that the width was mostly intrinsic and not due to Sr inhomogeneity, except for the sample at the lowest Sr content.¹² The Sr concentrations

estimated in this way turned out $x = 0.0185 \pm 0.0015$, 0.0315 ± 0.0015 and 0.0645 ± 0.002 , in good agreement with the nominal compositions. In the following the samples will be referred as $x = 0.019$, 0.03 and 0.06 .

The complex Young's modulus E was measured by electrostatically exciting either of the lowest three flexural modes and detecting the vibration amplitude by a frequency modulation technique. The elastic energy loss coefficient (or reciprocal of mechanical Q) is related to the imaginary part E'' of E by $Q^{-1}(\omega, T) = E''(\omega, T)/E'(\omega, T)$, and it was measured by the decay of the free oscillations or the width of the resonance peak.

In Fig. 1 the anelastic spectra of three samples with $x = 0.019$, 0.03 , 0.06 below 16 K measured exciting the first flexural mode are reported. A step-like increase of the absorption is observed around or slightly below T_g (Ref. 11) The gray arrows indicate the values of T_g in the magnetic phase diagrams deduced from NQR³ (lower values) and μSR ⁶ (higher values) experiments, which are in agreement with the data in Ref. 11 (for the sample with $x = 0.019$ the $T_g(x = 0.02)$ values are indicated). The black arrows indicate the temperature of the maximum of the ^{139}La NQR relaxation rate measured on the same samples in a separate study,¹³ which indicate a freezing in the spin-glass phase, as discussed later. The coincidence of the temperatures of the absorption steps with those of freezing of the spin fluctuations suggest a correlation between the two phenomena.

The sample with $x = 0.03$ was outgassed from excess O by heating in vacuum up to 790 K, while the other two samples were in the as-prepared state, therefore containing some interstitial O. The concentration δ of excess O is a decreasing function of x (Ref. 14) and should be negligible for $x = 0.06$ but not for $x = 0.019$. This fact allowed us to observe the absorption step singled out from the high-temperature tail of an intense peak that occurs at lower temperature (see the sharp rise of dissipation below 3 K for $x = 0.019$ in Fig. 1). Such a peak has been attributed to the tunneling-driven tilt motion of a fraction of the O octahedra.^{12,15} The LTO phase is inhomogeneous on a local scale,¹⁵⁻¹⁸ and a fraction of the octahedra would be unstable between different tilt orientations, forming tunneling systems which cause the anelastic relaxation process. The interstitial O atoms force the surrounding octahedra into a fixed tilt orientation, resulting in a decrease of the fraction of mobile octahedra and therefore in a depression of the absorption peak. In addition, doping shifts the peak to lower temperature at a very high rate, due to the coupling between the tilted octahedra and the hole excitations.¹² Therefore, it is possible to reduce the weight of the low temperature peak by introducing concentrations of interstitial O atoms that are so small that do not change appreciably the doping level due to the Sr substitutionals. Figure 2 compares the absorption curves of the $x = 0.019$ sample in the as-prepared state with a concentration $\delta \simeq 0.002$ of excess O and after removing it in vacuum at high temperature. The initial concentration δ has been estimated

from the intensity of the anelastic relaxation process due to the hopping of interstitial O,¹⁹ whose maximum occurs slightly below room temperature at our measuring frequencies (not shown here). The presence of excess O indeed decreases and shifts to lower temperature the tail of the peak in Fig. 2, while the effect on the absorption step is negligible. This justifies the comparison of the sample with $x = 0.019$ and $\delta > 0$ together with the other samples with $\delta \simeq 0$, and demonstrates that the nature of the low temperature peak is different from that of the step-like absorption.

III. DISCUSSION

The present data show the presence of a step in the acoustic absorption at the boundary of the spin-glass quasi-ordered state in the T, x magnetic phase diagram. The case of the $x = 0.019$ sample is less clear-cut, since the step is rather smooth. Furthermore, the Sr content is within the range $0.018 < x < 0.02$, at the boundary between the SG and the CSG phases, where the phase diagram is largely uncertain.¹³ The $T_f(x)$ line ends at 15 K for $x \simeq 0.018$, and the line $T_g(x)$ starts from 10-12 K at $x \simeq 0.02$ (Refs. 8,11,13). A larger spread of experimental data¹¹ (from 7.8 to 12.5 K) is actually observed just at $x = 0.02$.

A mechanism which in principle produces acoustic absorption is the slowing down of the magnetic fluctuations toward the spin-glass freezing. When measuring the spectral density $J_{\text{spin}}(\omega, T)$ of the spin fluctuations (the Fourier transform of the spin-spin correlation function), e.g. through the ¹³⁹La NQR relaxation rate, a peak in J_{spin} is found at the temperature at which the fluctuation rate $\tau^{-1}(T)$ becomes equal to the measuring angular frequency ω . Near the glass transition the magnetic fluctuation rate was found to approximately follow the law³ $\tau^{-1} \propto [(T - T_g)/T_g]^2$, and the temperature at which the condition $\omega\tau = 1$ for the maximum of relaxation is satisfied for $\omega/2\pi = 12 - 19$ MHz is close to T_g . A similar peak would be observed in the spectral density of the lattice strain $J_{\text{latt}}(\omega, T)$, if the spin fluctuations cause strain fluctuations through magnetoelastic coupling. The acoustic absorption is proportional to the spectral density of the strain and hence to J_{latt} , $Q^{-1} = \omega J_{\text{strain}}/T \propto \omega J_{\text{latt}}/T$, and therefore at our frequencies ($\omega \leq 50$ kHz) we should observe a narrow peak at a temperature slightly lower than the ones detected by NQR relaxation. The absorption steps in Fig. 1 can hardly be identified in a strict way as due to the contribution from the freezing magnetic fluctuations because they appear as steps instead of peaks. We propose that the main contribution comes from the stress-induced movement of the domain boundaries between the clusters of quasi-frozen antiferromagnetically correlated spins. The mechanism is well known for ferromagnetic materials,⁹ but is possible also for an ordered AF state,

if an anisotropic strain is coupled with the easy magnetization axis. In this case, the elastic energy of domains with different orientations of the easy axis would be differently affected by a shear stress, and the lower energy domains would grow at the expenses of the higher energy ones. The dynamics of the domain boundaries is different from that of the domain fluctuations and generally produces broad peaks in the susceptibilities. An example is the structural HTT/LTO transformation in the same samples, where the appearance of the orthorhombic domains is accompanied by a step-like increase of the acoustic absorption.²⁰ We argue that the features in the anelastic spectra just below T_g are associated with the stress-induced motion of the walls enclosing the clusters of AF correlated spins. More properly, the anelastic relaxation is attributed to the stress-induced changes of the sizes of the different domains.

The $x = 0.019$ sample is at the border $x_c \simeq 0.02$ between SG and CSG state. The NQR measurements on the same sample¹³ indicate a spin-freezing temperature ~ 9 K, closer to the CSG $T_g(x_c)$ rather than to the SG $T_f(x_c)$, which is consistent with the presence of moving walls, otherwise absent in the SG state. Nonetheless, following the model proposed by Gooding *et al.*²¹ we do not expect a sharp transition between the SG and the CSG states. According to that model, at low temperature the holes localize near the Sr dopants, and in the ground state an isolated hole circulates clockwise or anticlockwise over the four Cu atoms neighbors to Sr. Such a state induces a distortion of the surrounding Cu spins, otherwise aligned according to the prevalent AF order parameter. The spin texture arising from the frustrated combination of the spin distortions from the various localized holes produces domains with differently oriented AF order parameters, which can be identified with the frozen AF spin clusters. The dissipative dynamics which we observe in the acoustic response should arise from the fact that the energy surface of the possible spin textures has many closely spaced minima²¹ and the vibration stress, through magnetoelastic coupling, can favor jumps to different minima. In this picture, one could argue that the random distribution of Sr atoms may cause the formation of spin clusters also for $x \lesssim x_c$ and it is possible to justify the fact that for $x = 0.019$ the absorption step does not start below the maximum of the ¹³⁹La NQR relaxation rate, which signals the freezing of the spin clusters. Rather, the acoustic absorption slowly starts increasing slightly before the T_g determined by the NQR maximum is reached. This may indicate that the spin dynamics is not only governed by cooperative freezing, but is also determined by the local interaction with the holes localized at the surrounding Sr atoms. Then, the regions in which the Sr atoms induce a particularly strong spin-texture could freeze and cause anelastic relaxation before the cooperative transition to the glass state is completed. Systematic measurements around the $x = 0.02$ doping range are necessary to clarify this point.

The dependence of the intensity of the absorption step

on x , which is sharper and most intense at $x = 0.03$, qualitatively supports the above picture. In fact, at lower doping one has only few domains embedded in a long range ordered AF background, while above 0.05 the fraction of walls of disordered spins connecting the Sr atoms increases at the expenses of the ordered domains, with a cross-over to incommensurate spin correlations.²¹ The anelasticity due to the stress-induced change of the domain sizes is expected to be strongest in correspondence to the greatest fraction of ordered spins, namely between 0.03 and 0.05, in accordance with the spectra in Fig. 1.

Finally we point out the insensitiveness of the absorption step to the presence of interstitial O (Fig. 2 and Ref. 12), in view of the marked effects that even small quantities of excess O cause to the low temperature peak (Fig. 2) and to the rest of the anelastic spectrum.^{15,12} This is consistent with a dissipation mechanism of magnetic rather than of structural origin.

IV. CONCLUSION

The elastic energy loss coefficient of $\text{La}_{2-x}\text{Sr}_x\text{CuO}_4$ (proportional to the imaginary part of the elastic susceptibility) measured around 10^3 Hz in samples with $x = 0.019, 0.032$ and 0.064 shows a step-like rise below the temperature of the transition to a quasi-frozen cluster spin-glass state. The origin of the acoustic absorption is thought to be magnetoelastic coupling, namely anisotropic in-plane strain associated with the direction of the local staggered magnetization. The absorption is not peaked at T_g and therefore does not directly correspond to the peak in the dynamic spin susceptibility due to the spin freezing. Rather, it has been ascribed to the stress-induced changes of the sizes of the spin clusters, or equivalently to the motion of the walls. The phenomenology is qualitatively accounted for in the light of the model of Gooding *et al.*²¹ of magnetic correlations of the Cu^{2+} spins induced by the holes localized near the Sr dopants.

ACKNOWLEDGMENTS

The authors thank Prof. A. Rigamonti for useful discussions and for a critical review of the manuscript. This work has been done in the framework of the Advanced Research Project SPIS of INFM.

¹ A. Rigamonti, F. Borsa and P. Carretta, Rep. Prog. Phys. **61**, 1367 (1998).

² D. Vaknin, S.K. Sinha, D.E. Moncton, D.C. Johnston, J.M. Newsam, C.R. Safinya and H.E. King Jr., Phys. Rev. Lett. **58**, 2802 (1987).

- ³ J.H. Cho, F. Borsa, D.C. Johnston and D.R. Torgeson, Phys. Rev. B **46**, 3179 (1992).
- ⁴ F. Borsa, P. Carretta, J.H. Cho, F.C. Chou, Q. Hu, D.C. Johnston, A. Lascialfari, D.R. Torgeson, R.J. Gooding, N.M. Salem and K.J.E. Vos, Phys. Rev. B **52**, 7334 (1995).
- ⁵ M.-H. Julien, F. Borsa, P. Carretta, M. Horvati, C. Berthier and C.T. Lin, Phys. Rev. Lett. **83**, 604 (1999).
- ⁶ Ch. Niedermayer, C. Bernhard, T. Blasius, A. Golnik, A. Moodenbaugh and J.I. Budnick, Phys. Rev. Lett. **80**, 3843 (1998).
- ⁷ F.C. Chou, N.R. Belk, M.A. Kastner, R.J. Birgeneau and A. Aharony, Phys. Rev. Lett. **75**, 2204 (1995).
- ⁸ S. Wakimoto, S. Ueki, Y. Endoh and K. Yamada, cond-mat/9910400.
- ⁹ A.S. Nowick and B.S. Berry, *Anelastic Relaxation in Crystalline Solids*. (Academic Press, New York, 1972).
- ¹⁰ M. Daturi, M. Ferretti and E.A. Franceschi, Physica C **235-240**, 347 (1994).
- ¹¹ D.C. Johnston, *Handbook of Magnetic Materials*. ed. by K.H.J. Buschow, p. 1 (North Holland, 1997).
- ¹² F. Cordero, R. Cantelli and M. Ferretti, cond-mat/9910402, to be published in Phys. Rev. B.
- ¹³ A. Campana, R. Cantelli, M. Corti, F. Cordero and A. Rigamonti, unpublished.
- ¹⁴ E. Takayama-Muromachi and D.E. Rice, Physica C **177**, 195 (1991).
- ¹⁵ F. Cordero, C.R. Grandini, G. Cannelli, R. Cantelli, F. Trequattrini and M. Ferretti, Phys. Rev. B **57**, 8580 (1998).
- ¹⁶ D. Haskel, E.A. Stern, D.G. Hinks, A.W. Mitchell, J.D. Jorgensen and J.I. Budnick, Phys. Rev. Lett. **76**, 439 (1996).
- ¹⁷ E.S. Bozin, S.J.L. Billinge, G.H. Kwei and H. Takagi, Phys. Rev. B **59**, 4445 (1999).
- ¹⁸ F. Cordero, R. Cantelli, M. Corti, M. Campana and A. Rigamonti, Phys. Rev. B **59**, 12078 (1999).
- ¹⁹ F. Cordero, C.R. Grandini and R. Cantelli, Physica C **305**, 251 (1998).
- ²⁰ W.-K. Lee, M. Lew and A.S. Nowick, Phys. Rev. B **41**, 149 (1990).
- ²¹ R.J. Gooding, N.M. Salem, R.J. Birgeneau and F.C. Chou, Phys. Rev. B **55**, 6360 (1997); K.S.D. Beach and R.J. Gooding, cond-mat/0001095.

V. FIGURES CAPTIONS

Fig. 1 Elastic energy loss coefficient of $\text{La}_{2-x}\text{Sr}_x\text{CuO}_4$ with $x = 0.019$ (1.3 kHz), $x = 0.03$ (1.7 kHz), $x = 0.06$ (0.43 kHz). The gray arrows indicate the temperature T_g of freezing into the cluster spin-glass state deduced from NQR³ (lower values) and μSR ⁶ (higher values) experiments. The black arrows indicate the temperature of the maximum of the ¹³⁹La NQR relaxation rate measured on the same samples.¹³

Fig. 2 Elastic energy loss coefficient of the sample with $x = 0.019$ in the as prepared state (with interstitial O) and after outgassing the excess O measured at 1.3 kHz.

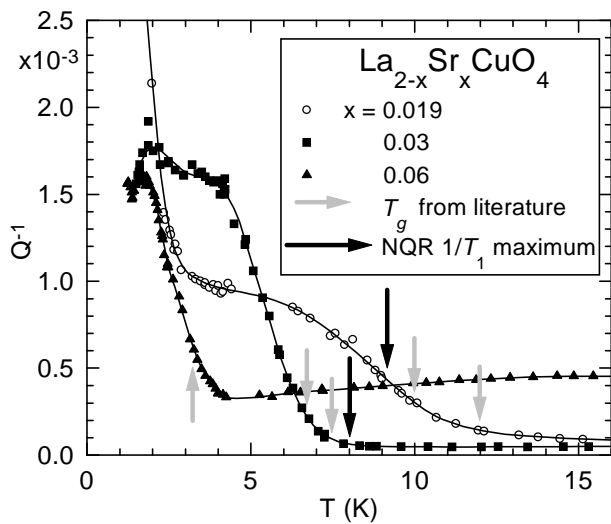


Fig. 1

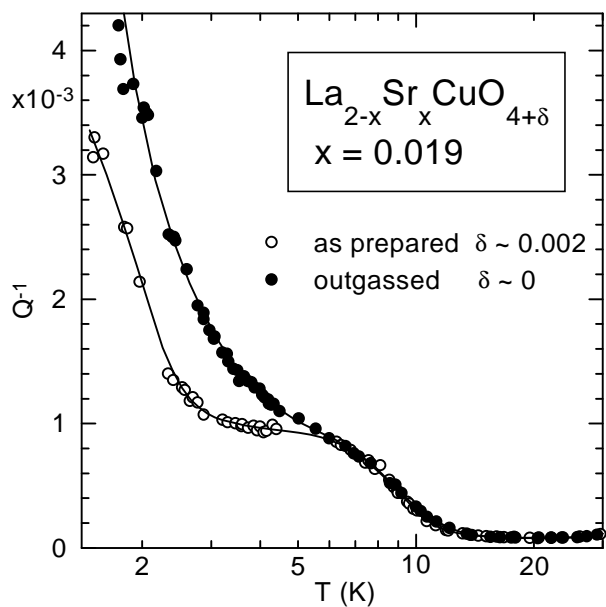


Fig. 2